SCIENTIFIC ARTICLE

Biomechanical Comparison of Volar Fixed-Angle Locking Plates for AO C3 Distal Radius Fractures: Titanium Versus Stainless Steel With Compression

Tyler Marshall, MD,* Amit Momaya, MD,* Alan Eberhardt, PhD,* Nilesh Chaudhari, MD,* Thomas R. Hunt III, MD†

Purpose To determine biomechanical differences between a fixed-angle locking volar titanium plate (VariAx; Stryker, Kalamazoo, MI) and a fixed-angle compression locking volar stainless steel plate (CoverLoc Volar Plate; Tornier, Amsterdam, Netherlands) in the fixation of simulated AO C3 distal radius fractures.

Methods Eighteen cadaveric upper extremities (9 matched pairs) with an average age of 54 years were tested. A 4-part AO C3 fracture pattern was created in each specimen. The fractures were reduced under direct vision and fixed with either the fixed-angle locking volar titanium plate or the fixed-angle compression locking volar stainless steel plate. Motion tracking analysis was then performed while the specimens underwent cyclic loading. Changes in displacement, rotation, load to failure, and mode of failure were recorded.

Results The fragments, when secured with the fixed-angle compression locking stainless steel construct, demonstrated less displacement and rotation than the fragments secured with the fixed-angle locking titanium plate under physiological loading conditions. In the fixed-angle compression locking stainless steel group, aggregate displacement and rotation of fracture fragments were 5 mm and 3° less, respectively, than those for the fixed-angle locking titanium group. The differences between axial loads at mechanical failure and stiffness were not statistically significant. The compression locking stainless steel group showed no trend in mode of failure, and the locking titanium plate group failed most often by articular fixation failure (5 of 9 specimens).

Conclusions The fixed-angle compression locking stainless steel volar plate may result in less displacement and rotation of fracture fragments in the fixation of AO C3 distal radius fractures than fixation by the fixed-angle locking volar titanium plate. However, there were no differences between the plates in mechanical load to failure and stiffness.

Clinical relevance Fixation of distal radius AO C3 fracture patterns with the fixed-angle compression locking stainless steel plate may provide improved stability of fracture fragments. *(J Hand Surg Am. 2015;■(■):■–■. Copyright © 2015 by the American Society for Surgery of the Hand. All rights reserved.)*

Key words Biomechanical analysis, distal radius fracture, locking, volar plate.

*From the *Division of Orthopedic Surgery, University of Alabama at Birmingham, Birmingham, AL; and the †Department of Orthopedic Surgery, Baylor College of Medicine, Houston, TX.*

Received for publication August 14, 2014; accepted in revised form June 16, 2015.

T.R.H. received royalties from Tornier and Wolters Kluwer/Lippincott Williams & Wilkins. Funding for this study was provided by Tornier (Saint-Ismier Cedex, France).

Corresponding author: Nilesh Chaudhari, MD, University of Alabama at Birmingham, 1313 13th St. South, Birmingham, AL 35205; e-mail: nchaudhari@uabmc.edu.

0363-5023/15/■ ■-0001$36.00/0
http://dx.doi.org/10.1016/j.jhsa.2015.06.098

Intra-articular fractures of the distal radius are complex injuries that require near-anatomical reduction to achieve successful outcomes. Complex intra-articular fracture patterns have been associated with difficult reduction and residual articular incongruity, particularly when volar and dorsal lunate facet fragments are present. Many authors have reported loss of initial fixation of the volar or dorsal lunate facet fracture fragments at short-term follow-up.[1–4] This is concerning because fracture displacement and articular stepoff greater than 2 mm have been linked to radiologically observed early posttraumatic arthritis in several studies,[1,3,4] although there remains debate about the consequences of residual articular displacement.[5] Appropriate treatment of these fractures should aim for stable, anatomical fixation that allows early motion.

Various treatment strategies have been employed in the fixation of distal radius fractures including percutaneous pinning, external fixation, volar and dorsal plating, and fragment-specific fixation.[6–12] Selection of the optimal treatment construct must take into account patient-specific factors, fracture pattern, and surgeon experience, and thus, no one method will be ideal for all distal radius fractures.

In recent years, volar plating has gained popularity. Anatomical fracture reduction using volar plates allows early motion and a reduction in tendon injuries associated with other methods of fixation.[13] Biomechanical studies have shown that many of the volar plating systems adequately stabilize extra-articular distal radius fractures.[6–8]

The purpose of this study was to mechanically evaluate 2 different volar plate designs in the fixation of simulated distal radius fractures with AO C3 fracture patterns with a fixed-angle locking volar titanium plate or a fixed-angle compression locking volar stainless steel plate. It was our hypothesis that the fractures fixed using the fixed-angle compression locking volar stainless steel plate would exhibit less interfragmentary displacement and rotation under physiological loading conditions owing to the increased friction at the bone-plate interface.[14,15]

MATERIALS AND METHODS

Specimen preparation

After obtaining institutional review board approval, 11 matched pairs of fresh-frozen cadaver upper extremities were obtained. Two of the matched pairs of cadavers were discarded and not used in the analysis owing to Kirschner (K)-wire slippage and inadequate data acquisition. Of the remaining 9 matched pairs, the average age was 54 years (range, 39–72 years). There were 8 male pairs and 1 female pair. None of the specimens had visual evidence of injury or surgery.

The left limbs were placed in the locking volar plate group (VariAx; Stryker, Kalamazoo, MI). The plate is composed of titanium. This construct has both a fixed-angle drill guide and a variable-angle drill guide, locking and nonlocking screws, and fully threaded and partially threaded screws. Only the fixed-angle drill guide with fully threaded screws was used.

The right limbs were placed in the fixed-angle compression locking group (CoverLoc Volar Plate; Tornier, Amsterdam, Netherlands). The plate is composed of stainless steel. The distal screws have nonthreaded heads, allowing the screw to continue turning in the hole to compress the bone fragment to the plate. A fixed-angle guide was used for the placement of all distal screws.

All extremities were thawed to room temperature and prepared in similar fashion. Soft tissue was stripped from the olecranon tip to 8 cm distally and from all 5 metacarpals to allow for potting. The distal radii were approached volarly and dorsally, stripping the skin and muscle tissues to allow for accurate data collection. Care was taken to leave the wrist capsule and ligamentous structures intact to allow for physiological loading conditions.

Fracture model

A 4-part AO C3 fracture was created in each of the specimens in an identical fashion. The technique was adapted from a previous study.[16] In order to accurately simulate fracture behavior under physiological loading conditions, all soft tissue attachments including the wrist ligaments and capsule were left in place. This is in contrast to some other studies, which eliminated soft tissue stabilizers from the carpus and distal radius.[6–8] A single investigator (T.M.) created the fractures and applied the plates to minimize variability. A 15-mm-wide dorsal wedge osteotomy was created using a sagittal saw 20 mm proximal to the articular surface to simulate comminution. The volar cortex was fractured manually to ensure anatomical reduction. A second osteotomy was created directly ulnar to the Lister tubercle in the sagittal plane. A third osteotomy was made coronally in the medial fragment to simulate a 4-part fracture. The coronal cut in the medial fragment was made from the fracture site to the articular surface of the radius. Each osteotomy in the medial fragment was designed to cut the fragment in half. The fractures were reduced under direct visualization, and the plates were applied. The fractures were then examined fluoroscopically to ensure adequate fixation and reduction (Fig. 1).

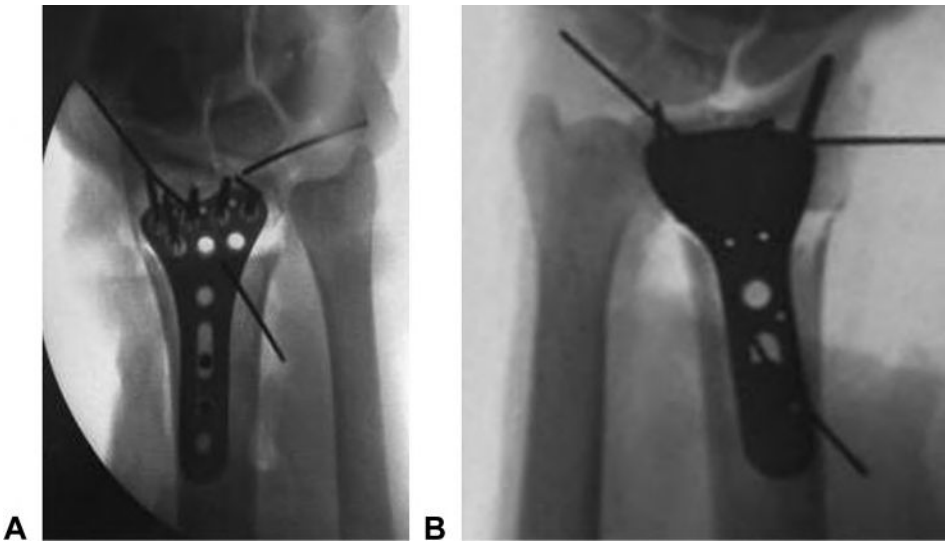

FIGURE 1: A Fluoroscopic image of a left-sided cadaveric specimen secured using the fixed-angle locking volar plate. **B** Fluoroscopic image of a right-sided cadaveric specimen secured using the fixed-angle compression locking volar plate.

Different plates were used for each specimen, and there was no reinsertion of screws.

Five distal screws and 2 proximal screws were placed in the fixed-angle locking plate. The distal locking screws were placed in the 2 slots for the radial styloid, and the remaining distal locking screws were placed in the distal-most row. These screws were positioned in a divergent manner as set by the plate. One proximal cortical screw was placed in the oblong shaft hole, and the other cortical screw was placed in the hole just proximal to it. All screws were fully threaded and 2.7 mm.

For the fixed-angle compression locking stainless steel plate, 5 distal screws and 2 proximal screws were placed. Two distal screws were placed in the radial styloid slots and the other 3 distal screws were placed in the distal-most row. These screws were positioned divergent as set by the plate. The distal screws were all 2.7 mm and fully threaded. Once the distal screws were fully seated, the locking sheath was placed, creating a locked, fixed-angle construct. One proximal cortical screw was placed in the oblong hole, and another cortical screw was placed in the proximal most hole. The proximal screws were 3.3 mm and fully threaded.

Loading protocol and data collection

Four 1.6-mm K-wires were placed into the fracture fragments: 2 in the medial fragments, 1 in the radial styloid, and 1 in the radial shaft. The K-wire in the radial shaft served as the control and was placed volarly. The other K-wires were placed dorsally except for the volar medial fragment in which the K-wires were placed volarly. Reflective triad markers were attached to each of the K-wires for motion tracking purposes. A cyclic load was applied using a materials testing machine (MTS, Gothenburg, Sweden) to mimic normal physiological loading conditions associated with wrist motion. A preload of 100 N was applied followed by cyclic loading from 20 N to 230 N at 2 Hz for 6,000 cycles.[7,8] A target load of 250 N was chosen because it represents the force the tendons exert on the radius during wrist range of motion or when clenching a fist.[17] However, the target load was not achieved owing to issues with the testing tuning. In cyclic load control, the loads do not always reach their intended value. This is due to testing and tuning. The motion of the triads during the 6,000 cycles was recorded using motion tracking software. Each sample was then loaded to failure at a rate of 2 mm/s, where failure was defined by a significant drop in the force applied during the displacement controlled loading. The force at failure was measured along with the stiffness, which was determined as the slope of the linear portion of the load-displacement response during the final loading phase. The mode of failure for each specimen was also recorded.

A 3-camera setup, consisting of a MCU 1000 ProReflex camera and 2 MCU 120 ProReflex cameras (Qualisys, Gothenburg, Sweden), was used to track the motion of each triad so that 2 cameras were able to see each marker at all times. The camera system was calibrated before each testing session using a standard calibration kit with a custom-built apparatus to hold the frame at the same location for each testing session. Qualisys Motion Capture Systems' Qualisys Track Manager (Gothenburg, Sweden) software was used for the calibration and to record

TABLE 1. Motion Tracking Data for Each Specimen

Specimen Number	Aggregate Displacement (mm)		Aggregate Rotation (°)	
	Compression Locking	Locking	Compression Locking	Locking
1	11.3	9.7	6.0	6.7
2	10.8	14.3	4.2	7.0
3	8.7	16.3	3.3	6.5
4	9.8	15.0	4.4	10.1
5	12.0	19.6	6.1	6.3
6	8.9	19.0	3.5	10.9
7	30.4	28.5	10.7	10.4
8	8.9	11.0	3.9	5.1
9	8.2	18.6	3.0	8.1
Mean	12.1	16.9	5.0	7.9
SD	7.0	5.6	2.4	2.1
Standard error	2.3	1.9	0.8	0.7

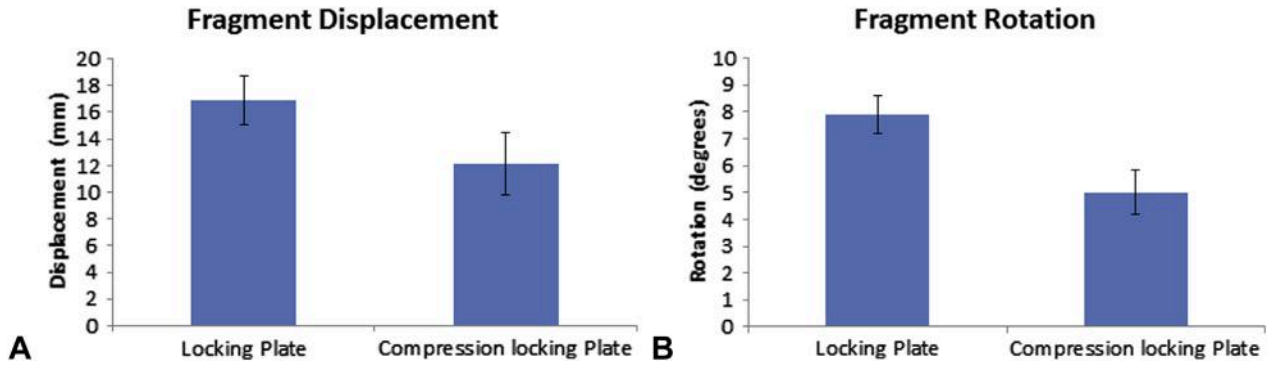

FIGURE 2: Differences in motion between fixation with the locking plate versus the compression locking plate. Shown are the averages for the summed displacement (mm) **A** and summed rotations (degrees) **B** for each sample.

triad motion during testing at 120 Hz. Rigid bodies were defined in the Qualisys Track Manager software for each marker triad. The kinematic data were computed relative to the global camera coordinate system that was aligned with the radius with the z axis parallel to the long axis of the radius. The displacement values in the x, y, and z planes for the fracture fragments were added to compute the aggregate displacement. Similarly, rotation values of the fragments were summed to find the aggregate rotation.

Statistical analysis

The sum of the relative displacements and the sum of the relative rotations of the 3 fragments for each specimen were calculated. Paired *t* tests were performed to compare the summed displacements and rotations between paired wrists to compare the 2 plate types. *P* values of less than .05 were considered statistically significant. The Fisher exact test was used to compare modes of failure for the 2 groups.

RESULTS

Cyclic testing

The aggregate displacement and rotation between the 2 groups for each specimen are shown in Table 1. Significant differences between the fixed-angle locking titanium plate and the fixed-angle compression locking stainless steel plate were seen both in the amount of displacement ($P = .015$) and the amount of rotation ($P = .013$) between the 2 plate types. In the fixed-angle compression locking stainless steel group, the average aggregate fragment displacement per specimen was 4.8 mm less than that of the fixed-angle locking titanium group. The average aggregate rotation per specimen was 3° less in the fixed-angle compression locking stainless steel group than in the fixed-angle locking titanium

TABLE 2. Load to Failure and Stiffness for Each Specimen

Specimen Number	Load at Failure (N)		Stiffness (N/mm)	
	Compression Locking	Locking	Compression Locking	Locking
1	881	1,114	171	513
2	1,033	1,244	518	371
3	997	828	570	111
4	1,049	844	444	433
5	2,270	1,567	670	609
6	2,353	631	704	354
7	631	1,027	201	238
8	1,194	1,310	342	342
9	1,598	1,414	377	437
Mean	1,334	1,109	444	379
SD	611	305	190	146
Standard error	204	102	63	49

TABLE 3. Mode of Failure for Each Specimen

Mode of Failure	Compression Locking	Locking	All
Articular fixation failure	1	5	6
Plate buckle	3	1	4
Proximal screw pull-out	1	2	3
Undetermined	4	1	5

group. A comparison of the mean displacement and rotation of the 2 groups is shown in Figure 2.

Load to failure

The axial load at mechanical failure and stiffness during axial loading for each specimen are summarized in Table 2. The differences between axial loads at mechanical failure and stiffness were not statistically significant. The types of failure for each specimen are reported in Table 3. The locking titanium plate failed by articular fixation failure in 5 of 9 specimens. The compression locking stainless steel plate group showed no trend in mode of failure, but as a comparison failed only 1 of 9 times by failure of articular fixation. The differences in mode of failure were not statistically significant.

DISCUSSION

Volar plate fixation has been popularized in recent years based on practical and theoretical benefits. Ease of application, early return of upper limb function, and decreased complications have made volar plate fixation an attractive option for treating distal radius fractures.[18,19] This study focused on specific mechanical differences using 2 different volar plate constructs. The fracture pattern studied has been associated with early failure of fixation and poor patient outcomes.[3,4]

The fixed-angle locking titanium volar plate relies on load bearing through the locked plate-screw construct for maintenance of reduction. The fixed-angle compression locking volar stainless steel plate allows for the addition of a compression effect created by the non-threaded screw head, which allows the screws to continue to turn in the hole and pull the bone to the plate, thus increasing friction at the bone-plate interface. Another variable that may have contributed to differences in fixation between the 2 plates was the differences in the fixed-angle screw trajectories. However, such variations in fixed-angle patterns are unlikely to account for the overall differences in fixation.

Although the aggregate displacement for the fracture fragments may seem high under physiological loads, these measurements were the aggregate of 6,000 cycles. Furthermore, the measurements were taken from the markers on the K-wires, and thus, it is possible that the motion measured was greater than the actual motion between the fracture fragments. However, the same K-wires and setup were used for each specimen, and so such variables were controlled.

Multiple authors have demonstrated difficulty in the treatment of these injuries. Harness et al[3] report 4 out of 7 patients with volar lunate facet fractures had early failure of fixation and required reoperation. Bradway et al[4] reported 16 intra-articular distal radius fractures in which all patients with a stepoff greater than 2 mm developed posttraumatic arthritis.

Multiple authors also have examined the biomechanical stability of volar plating compared with other constructs. Leung et al[20] compared traditional volar plating, locked volar plating, and dorsal plating for AO C2 fractures in a cadaveric model. All plates were made from stainless steel. They found that the volar locked plate was biomechanically superior to the traditional plate and dorsal plate systems. Taylor et al[11] found that, in a cadaveric AO C2 type model, volar locking plate constructs compared similarly with fragment-specific fixation under physiological loads. Martineau et al[21] compared the use of locking screws with smooth locking pegs on an AO C3 cadaveric fracture model and found that locking screws provided optimal construct stability, particularly in relation to the ulnar-sided fragment. Osada and Viegas[7] demonstrated that volar plate fixation compared favorably and may offer a biomechanical advantage to dorsal plating for fixation of extra-articular fractures in a cadaveric model. Koh and Viegas[6] concluded in a cadaveric biomechanical study that volar plate fixation of extra-articular distal radius fractures delivered sufficient stability to possibly allow patients mobilization and wrist range of motion as early as 1 week after surgery.

A limitation in the study relates to the standardization of the fracture model. Every attempt was made to reproduce the fracture model in each cadaver specimen by using one investigator. Also, standardized cuts were made by the sagittal saw based upon measurements. However, it was difficult to identically reproduce the fracture model in each specimen.

Another potential weakness of this study was that the plating systems used are made of different materials. The fixed-angle locking plate is titanium and the fixed-angle compression locking plate is stainless steel. This difference could contribute to a greater stiffness of the isolated fixed-angle compression locking plate. Plating systems made of the same material were not available. Furthermore, potential differences in the forces and stiffness are not simply due to material differences but also to geometry differences. Nonetheless, we feel that the main outcome of this study, examining fracture displacement under physiological loads, should be unaffected by this difference. Souer et al[22] demonstrated no difference between a titanium plate and a stainless steel plate with regard to functional outcome. Moreover, the failures of the fixation observed were most often secondary to loss of screw fixation and not related to plate breakage and failure.

A possible confounding variable involves the laterality of the distal radius used for each plate construct. The left distal radii were used for the locking plates and the right and presumably dominant distal radii were used for the compression locking plates. A previous study documented increased bone mineral content at the distal radius in the dominant compared with the nondominant arms in female volleyball players.[23] However, no studies have documented significant differences in bone mineral density or bone mineral content at the distal radius related to handedness in older adults.

Other limitations relate to the age and sex demographics of the cadaver specimens. The mean age of the specimens was 54 years, and thus, it is difficult to extrapolate our findings to younger or older patients. Also, including more female cadaver specimens would have strengthened the study.

Further research is necessary to determine if these results are of clinical importance.

REFERENCES

1. Knirk JL, Jupiter JB. Intra-articular fractures of the distal end of the radius in young adults. *J Bone Joint Surg Am*. 1986;68(5):647–659.
2. Orbay JL, Fernandez DL. Volar fixation for dorsally displaced fractures of the distal radius: a preliminary report. *J Hand Surg Am*. 2002;27(2):205–215.
3. Harness NG, Jupiter JB, Orbay JL, Raskin KB, Fernandez Dl. Loss of fixation of the volar lunate facet fragment in fractures of the distal part of the radius. *J Bone Joint Surg Am*. 2004;86(9):1900–1908.
4. Bradway J, Amadio P, Cooney W. Open reduction and internal fixation of displaced, comminuted intra-articular fractures of the distal end of the radius. *J Bone Joint Surg Am*. 1989;71(6):839–847.
5. Marsh JL, Buckwalter J, Gelberman R, et al. Articular fractures: does an anatomic reduction really change the result? *J Bone Joint Surg Am*. 2002;84(7):1259–1271.
6. Koh S, Viegas S. Volar fixation for dorsally angulated extra-articular fractures of the distal radius: a biomechanical study. *J Hand Surg Am*. 2006;31(5):771–779.
7. Osada D, Viegas S. Comparison of different distal radius dorsal and volar fracture fixation plates: a biomechanical study. *J Hand Surg Am*. 2003;28(1):94–104.
8. Windolf M, Schwieger K. A novel non-bridging external fixator construct versus volar angular stable plating for the fixation of intra-articular fractures of the distal radius: a biomechanical study. *Injury*. 2010;41(2):204–209.
9. Alffram PA, Bauer GC. Epidemiology of fractures of the forearm: a biomechanical investigation of bone strength. *J Bone Joint Surg Am*. 1962;44:105–114.
10. Grindel SI, Wang M, Gerlach M, McGrady LM, Brown S. Biomechanical comparison of fixed-angle volar plate versus fixed-angle volar plate plus fragment-specific fixation in a cadaveric distal radius fracture model. *J Hand Surg Am*. 2007;32(2):194–199.
11. Taylor KF, Parks BG, Segalman KA. Biomechanical stability of a fixed-angle volar plate versus fragment-specific fixation system: cyclic testing in a C2-type distal radius cadaver fracture model. *J Hand Surg Am*. 2006;31(3):373–381.
12. Cooper EO, Segalman KA, Parks BG, Sharma KM, Nguyen A. Biomechanical stability of a volar locking-screw plate versus fragment-specific fixation in a distal radius fracture model. *Am J Orthop*. 2007;36(4):46–49.
13. Wei J, Yang TB, Luo W, Qin JB, Kong FJ. Complications following dorsal versus volar plate fixation of distal radius fracture: a meta-analysis. *J Int Med Res*. 2013;41(2):265–275.
14. Stoffel K, Deiter U, Stachowiak G, Gachter A, Kuster MS. Biomechanical testing of the LCP—how can stability in locked internal fixators be controlled? *Injury*. 2003;34(Suppl 2):B11–B19.

15. Stoffel K, Klaue K, Perren SM. Functional load of plates in fracture fixation in vivo and its correlate in bone healing. *Injury*. 2000;31(Suppl 2):S-B37−S-B50.
16. Windolf M, Schwieger K, Ockert B, Jupiter JB, Gradl G. A novel non-bridging external fixator construct versus volar angular stable plating for the fixation of intra-articular fractures of the distal radius—a biomechanical study. *Injury*. 2010;41(2):204−209.
17. Putnam MD, Meyer NJ, Nelson EW, Gesensway D, Lewis JL. Distal radius metaphyseal forces in an extrinsic grip model: implications for postfracture rehabilitation. *J Hand Surg Am*. 2000;25(3):469−475.
18. Cooney WP, Dobyns JH, Linscheid RL. Complications of Colles' fractures. *J Bone Joint Surg Am*. 1980;62(4):613−619.
19. Shin EK, Jupiter JB. Current concepts in the management of distal radius fractures. *Acta Chir Orthop Traumatol Cech*. 2008;74(4):233−246.
20. Leung F, Zhu L, Ho H, Lu WW, Chow SP. Palmar plate fixation of AO type C2 fracture of distal radius using a locking compression plate—a biomechanical study in a cadaveric model. *J Hand Surg Br*. 2003;28(3):263−266.
21. Martineau PA, Waitayawinyu T, Malone KJ, Hanel DP, Trumble TE. Volar plating of AO C3 distal radius fractures: biomechanical evaluation of locking screw and locking smooth peg configurations. *J Hand Surg Am*. 2008;33(6):827−834.
22. Souer JS, Ring D, Matschke S, Audige L, Maren-Hubert M, Jupiter J. Comparison of functional outcome after volar plate fixation with 2.4 mm titanium versus 3.5 mm stainless-steel plate for extra-articular fracture of the distal radius. *J Hand Surg Am*. 2010;35(3):398−405.
23. Alfredson H, Nordstrom P, Pietila T, Lorentzon R. Long-term loading and regional bone mass in the arm in female volleyball players. *Calcif Tissue Int*. 1998;62(4):303−308.